Photodetachment of H^- with excitation to $H(N=2)$

M. Cortés and F. Martín
Departamento de Química C-14, Universidad Autónoma de Madrid, 28049-Madrid, Spain
(Received 5 April 1993)

We have applied a recently proposed L^2 method to evaluate total and partial photodetachment cross sections of H^- up to the $N=3$ threshold. The method was specially designed to evaluate continuum states when interchannel coupling is very strong, so that the H^- ion is an ideal system to test its validity. The calculated cross sections exhibit two Feshbach resonances below $N=2$, the well-known shape resonance just above the threshold, and five Feshbach resonances converging to $N=3$. The structure of these resonances is analyzed in detail, as well as the behavior of the partial cross sections in these regions. We also provide a complete set of Fano and Starace parameters that are useful to interpret the total and partial photodetachment spectra in the resonance regions. Finally, our results are compared with the available experimental data as well as with other theoretical calculations.

PACS number(s): 32.80.Fb, 32.80.Dz, 31.50.+w

I. INTRODUCTION

The H^- ion is the two-electron system with the lowest nuclear charge in the helium isoelectronic series. It is also the simplest negative ion, so that it is used as a prototype to understand the physics of such weakly bound systems. As the nuclear charge, Z, is smaller than the number of electrons turning around, the H^- ion has specific properties which make it different from other heliumlike systems: the electron-electron interaction is as strong as the nucleus-electron one, and therefore the motion of the electrons is highly correlated, especially for continuum states. Indeed, the nature of the continuum states of H^- is governed by the long-range interaction between one electron and a neutral hydrogen atom. The former induces a "permanent" dipole, which results in a strong mixing between degenerate angular momentum states, i.e., in a strong correlated motion for the electrons [1–3]. Therefore, in the photodetachment of H^- above the $N=2$ threshold, the interchannel coupling between continuum states associated to the $2s$ and $2p$ states of neutral hydrogen is very strong.

In addition to the usual Feshbach resonances that are common to any two-electron system, the H^- ion also exhibits shape resonances. Their existence can be inferred from an analysis of the long-range dipole interaction mentioned above [4], and shows that electron correlation is essential for their description. Also, such an analysis explains why some series of Feshbach resonances that are present for $Z \geq 2$, are absent in H^-.

Finally, the H^- ion is an ideal system to perform multiphoton experiments. Indeed, as it has only one bound state, transitions to other intermediate bound states are not possible, thus simplifying the analysis of the resulting spectra.

All these peculiarities make the continuum of H^- very attractive for experimentalists and theoreticians, who have devoted some effort in order to describe it quantitatively.

In one-photon absorption experiments, ionization is described by continuum states of $^1P^o$ symmetry. Therefore, only resonance states of that symmetry are populated, which permits a clear identification of the structures observed in the spectra. Bryant *et al.* [5,6] and Halka *et al.* [7] have measured the total photodetachment cross sections of H^- near the $N=2$ threshold. The corresponding spectra show clearly the first $^1P^o$ Feshbach resonance just below the first ionization threshold, and the well-known $^1P^o$ shape resonance just above $N=2$. Hamm *et al.* [8] and Cohen *et al.* [9] have obtained total photodetachment cross sections near $N=3$, thus providing useful experimental information on the doubly excited states lying in this region. Harris *et al.* [10] have extended this kind of experiment to more excited thresholds. Only very recently, Halka *et al.* [7,11] have been able to provide partial photodetachment cross sections by observing the partial decay into $H(N=2)$ near the $N=2$ [7], $N=3$ [11], and $N=4$ [11] thresholds. As far as we know, this is the only experimental information concerning partial cross sections in H^-.

Theoretical calculations of photodetachment cross sections are relatively few, and are mainly concentrated in the vicinity of the $N=2$ threshold. We should mention the early close-coupling calculations of Macek [12] and Hyman, Jacobs, and Burke [13], which explicitly showed the existence of the $^1P^o$ shape resonance just above $N=2$. Based on the J-matrix method [14], Broad and Reinhardt [15] performed more sophisticated calculations, which also revealed the presence of the $^1P^o$ Feshbach resonance below that threshold. More recently, Liu, Du, and Starace [16] have obtained cross sections in the shape resonance region, using adiabatic hyperspherical representations of the channel functions. Although these theories agree in predicting the existence of the shape resonance, no two theories have similar predictions for the width, the form, and the position of the maximum of the resonance, especially for partial cross sections. Unfortunately, the experiments do not provide absolute cross sections and, therefore, more theoretical effort in this energy region seems to be appropriate.

On the other hand, Burkov, Letyaev, and Strakhova [17] have obtained photodetachment cross sections near $N=3$, and Sadeghpour, Greene, and Cavagnero [18] have carried out an extensive calculation of total and partial photodetachment cross sections up to the $N=4$ threshold. These two calculations were performed with the R-matrix method [19] and provided the Fano parameters [20] for some resonances lying below $N=3$.

Additional theoretical effort has been devoted to the evaluation of the energy positions and the total autoionization widths of the $^1P^o$ resonances of H^-. Calculations for the lowest Feshbach resonances that lie below $N=2$ are numerous (see for instance [21–28], and references therein). Much scarcer are the results for the resonances converging to the $N=3$ threshold [26,29–33]. From the latter works, only Chrysos, Komninos, and Nicolaides [33] have provided partial widths, exclusively for the first Feshbach resonance of the series. Also, there exist some theoretical calculations for the parameters of the shape resonance [23,26,30], but no one has provided partial widths or the Fano and Starace parameters.

In this paper, we complete the previous works by calculating the total and partial photodetachment cross sections of H^- up to the $N=3$ threshold. In this respect, we provide additional information on partial autoionization widths, and the set of Fano [20] and Starace parameters [34], which are useful to interpret the resonance structures observed in the total and partial cross section spectra, respectively.

For this purpose we have used a fully L^2 method [35], which has been specially designed to evaluate continuum states when interchannel coupling is very strong. This is a challenge for the use of L^2 techniques, which must provide continuum wave functions with the correct δ-function normalization and the proper boundary conditions, in order to correctly introduce the couplings. The method of Ref. [35] is based on the Feshbach formalism [36] and is a generalization of the works of Sánchez and Martín [37–39] on the photoionization of the helium atom below $N=3$. These authors proposed the use of a set of discretized uncoupled continuum states to solve the K-matrix scattering equations and to obtain the nonresonant continuum Green function [38]. In practice, the continuum wave function is expressed in terms of Slater-type orbitals (STO's), so that matrix elements are easily evaluated. The coupling between uncoupled continuum states is introduced by simply solving a system of linear equations [35], thus avoiding the numerical solution of the corresponding system of differential equations. This work is the first application of the method of Ref. [35] to the H^- ion.

The paper is organized as follows. In Sec. II we briefly outline the main features of the theoretical method proposed in [35], and describe in some detail its implementation for the study of the photodetachment of H^-. The total and partial photodetachment cross sections are presented in Sec. III, and are compared with previous theoretical and experimental works. In this section we also provide resonance parameters for the doubly excited states of H^- that lie below the $N=3$ threshold and briefly discuss the fitting procedure used to obtain such parameters in the shape resonance region. In Sec. IV, we end with some conclusions.

Atomic units are used throughout the paper unless otherwise stated.

II. THEORETICAL METHOD

The ground state of H^- has been obtained by diagonalizing the Hamiltonian in a basis of 130 configurations built from STO's. The exponents of the basis have been selected by imposing minimization of the energy and verification of the virial theorem. Our calculated energy is $-0.527\,542$ a.u. to be compared with the "exact" nonrelativistic value, $-0.527\,751$ a.u., of Pekeris [40].

There are four open channels below $N=3$: $\mu=1s\varepsilon p$, $2s\varepsilon p$, $2p\varepsilon s$, and $2p\varepsilon d$. For each channel μ, the exact continuum wave function $\psi^-_{\mu E}$ is written [38] as

$$|\psi^-_{\mu E}\rangle=\frac{\langle\phi_s|Q\mathcal{H}P|P\psi^{0-}_{\mu E}\rangle}{E-\mathcal{E}_s-\Delta_s(E)-i[\Gamma_s(E)/2]}|\phi_s\rangle +[1+G^{(s)}_Q(E)Q\mathcal{H}P]\left[|P\psi^{0-}_{\mu E}\rangle+\frac{\langle\phi_s|Q\mathcal{H}P|P\psi^{0-}_{\mu E}\rangle}{E-\mathcal{E}_s-\Delta_s(E)-i[\Gamma_s(E)/2]}G^{(s)-}_P(E)P\mathcal{H}Q|\phi_s\rangle\right], \tag{1}$$

where P and Q are the usual two-electron Feshbach projection operators [36,41]:

$$P=P_1+P_2-P_1P_2\ , \tag{2}$$

$$Q=1-P\ , \tag{3}$$

ϕ_s is the resonant wave function of energy $\mathcal{E}_s$ which is the solution of a projected Schrödinger equation in the Q subspace, $G^{(s)}_Q(E)$ is the Green operator in Q subspace in which the s state has been excluded, $P\psi^{0-}_{\mu E}$ is a nonresonant wave function of energy E which is the eigenstate of $P\mathcal{H}P+P\mathcal{H}QG^{(s)}_Q(E)Q\mathcal{H}P$, $G^{(s)-}_P(E)$ is the corresponding Green operator in P subspace, $\Gamma_s(E)$ is the "width," and $\Delta_s(E)$ is the "shift" of the ϕ_s resonance at the energy E.

Although Eq. (1) is exact, the way of writing $\psi^-_{\mu E}$ is not unique. Indeed, we can obtain an equivalent representation of $\psi^-_{\mu E}$ by selecting a different ϕ_r state, and hence different $G^{(r)}_Q(E)$ and $G^{(r)-}_P(E)$ functions. This flexibility allows one to single out any ϕ_s state to write Eq. (1) and, in particular, the ϕ_s state that is closer to the s Feshbach resonance in order to accelerate convergence in the calculation of $G^{(s)}_Q(E)$ and $G^{(s)-}_P(E)$.

Consequently, near the $N=3$ threshold we have used

$$P_i=\sum_{N=1}^{N_T}\sum_{l=1}^{N-1}\sum_{m=-l}^{l}|\varphi_{Nlm}(i)\rangle\langle\varphi_{Nlm}(i)|\ , \tag{4}$$

with $N_T=2$, which includes all $N=1$ and $N=2$ states of hydrogen, so that the lowest ϕ_s wave functions approximately represent the $3lnl'$ doubly excited states of H^-. More precisely, channels associated to $N\geq 3$ appear in Q subspace, and are taken into account in the calculations through the $G_Q^{(s)}(E)$ operator.

On the other hand, there is no ϕ_s state that could be related to the shape resonance that lies just above the $N=2$ threshold. Indeed, shape resonance components do not appear in Q subspace, but in P subspace. In particular, if P_i is given by Eq. (4), $\simeq 90\%$ of the shape resonance normalization belongs to P. This percentage increases if one includes more terms in Eq. (4). Therefore, the particular form of Q (hence of P) is irrelevant for practical purposes when one tries to evaluate the continuum wave function $\psi_{\mu E}^-$ in the vicinity of the $N=2$ threshold. In this energy region we have used the P_i projection operator of Eq. (4) with $N_T=3$. Then, the summation in Eq. (4) includes all $N=1$, $N=2$, and $N=3$ states of hydrogen, which are associated with the strongest interacting channels in that region. Therefore, channels with $N\geq 4$ are obtained in Q subspace and are included through the $G_Q^{(s)}(E)$ operator.

Therefore, in order to obtain the continuum state of Eq. (1) in one case or the other, we need to evaluate two kinds of wave functions, ϕ_n and $P\psi_{\mu E}^{0-}$, and the corresponding Green operators, $G_Q^{(s)}(E)$ and $G_P^{(s)-}(E)$. The ϕ_n wave functions have been evaluated in the framework of the pseudopotential-Feshbach method [42]. The corresponding Schrödinger equation has been solved in a representation of 335 configurations built from a basis of STO's which has been optimized using a minimum energy criterion. The basis includes STO's from $n=1$ to $n=10$, and angular momenta from $l=0$ to $l=4$, and is appropriate to represent the lowest Feshbach resonances lying below $N=2$, $N=3$, and $N=4$. The expansion of $G_Q^{(s)}(E)$ includes the first 120 eigenfunctions of $Q\mathcal{H}Q$, that represent $nln'l'$ doubly excited states with $n,n'>N_T$, and discretized $nl\varepsilon l'$ continuum functions with $n>N_T$ which our basis is able to reproduce. Although convergence in $G_Q^{(s)}(E)$ is accelerated by selecting in Eq. (1) the ϕ_s wave function that is closer to the s resonance, we have found that such a large number of states is necessary in order to properly describe polarization effects in H^- especially near the $N=3$ threshold.

The Green function $G_P^{(s)-}(E)$ is obtained in a basis of orthogonal L^2 uncoupled states $\tilde{\chi}_{\mu n}^0$, which belong to P subspace, by solving the system of linear equations:

$$\sum_{\mu'',n''}\mathcal{C}_{\mu'n'\mu''n''}\langle\tilde{\chi}_{\mu''n''}^0|G_P^{(s)-}(E)|\tilde{\chi}_{\mu n}^0\rangle=\mathcal{D}_{\mu'n'}\ , \tag{5}$$

where the coefficients $\mathcal{C}_{\mu'n'\mu''n''}$ and $\mathcal{D}_{\mu'n'}$ are given by

$$\mathcal{C}_{\mu'n'\mu''n''}=\delta_{\mu''\mu'}\delta_{n''n'}-\Xi_{\mu'}(E_{n'})\langle\tilde{\chi}_{\mu'n'}^0|V|\tilde{\chi}_{\mu''n''}^0\rangle\ , \tag{6}$$

$$\mathcal{D}_{\mu'n'}=\delta_{\mu'\mu}\delta_{n'n}\Xi_{\mu'}(E_{n'})\ , \tag{7}$$

$\{\tilde{\chi}_{\mu n}^0\}$ is a complete set of orthogonal L^2 uncoupled-continuum wave functions, which are solutions of single-channel Schrödinger equations, V is the interaction potential that includes the interchannel couplings and the polarization potential [38], and

$$\Xi_{\mu'}(E_{n'})=\begin{cases}i\pi\rho_{\mu'}(E_{n'}) & \text{for } E_{n'}=E_n\\ 1/(E_n-E_{n'}) & \text{for } E_{n'}\neq E_n\end{cases}\ , \tag{8}$$

where $\rho_\mu(E_n)$ is the square of the appropriate renormalization factor for the $\tilde{\chi}_{\mu n}^0$ functions to be properly δ normalized. Equation (5) represents a system of linear equations in the complex plane for each μ. (According to our choice for the projection operator P discussed above, μ runs over $1s\varepsilon p$, $2s\varepsilon p$, $2p\varepsilon s$, and $2p\varepsilon d$ near $N=3$, whereas μ runs over $1s\varepsilon p$, $2s\varepsilon p$, $2p\varepsilon s$, $2p\varepsilon d$, $3s\varepsilon p$, $3p\varepsilon s$, $3p\varepsilon d$, $3d\varepsilon p$, and $3d\varepsilon f$ near $N=2$, which leads to four and nine systems of linear equations, respectively.) The coefficient matrix **C** multiplying the unknowns is the same for all μ, so that each system of equations differs exclusively in the right-hand side column vector **D**. Therefore, only one matrix inversion is required to solve Eq. (5).

The L^2, $\tilde{\chi}_{\mu n}^0$ states are evaluated with an even-tempered basis of STO's using the standard codes of Macías *et al.* [43], which also provide the renormalization factors $\rho_\mu(E_n)$ for each μ and each energy E_n.

Then, for all μ associated to open channels, the $P\psi_{\mu E}^{0-}$ nonresonant wave function is written as

$$P\psi_{\mu E_n}^{0-}=\rho_\mu^{1/2}(E_n)\left[\tilde{\chi}_{\mu n}^0+\sum_{\mu',n'}\sum_{\mu'',n''}\langle\tilde{\chi}_{\mu''n''}^0|G_P^{(s)-}(E_n)|\tilde{\chi}_{\mu'n'}^0\rangle\langle\tilde{\chi}_{\mu'n'}^0|V|\tilde{\chi}_{\mu n}^0\rangle\tilde{\chi}_{\mu''n''}^0\right]\ . \tag{9}$$

The cross sections have been evaluated, using the ground state and the continuum wave functions described above, in the dipole approximation for photon energies between 10.75 and 12.85 eV. An energy grid with variable step size has been used in order to exhibit the whole resonant structure. All calculations have been done in quadruple precision.

III. RESULTS AND DISCUSSION

A. General aspects of the cross sections

We show in Fig. 1 an overview of the total photodetachment cross sections calculated in both the length and the velocity representations. Gauge invariance is very good, thus showing that the basis sets used to represent the continuum wave function in Eq. (1) are almost complete in this energy range. This is a general conclusion for all the results that will be presented below, and, therefore, will not be referred to anymore.

As can be observed in Fig. 1, the cross section varies smoothly with the photon energy, except in the vicinity of the $N=2$ and $N=3$ thresholds, where several resonant structures are apparent. Just below $N=2$, one can see two narrow Feshbach resonances. Only the first one has been detected experimentally [5,7,44], whereas the second is probably too narrow to be observed. The latter reso-

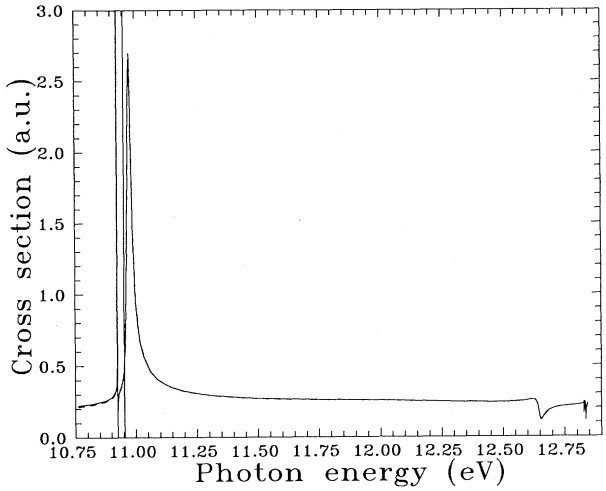

FIG. 1. Total photodetachment cross section of H^-. ——, length gauge; — — —, velocity gauge. The $N=2$ and $N=3$ thresholds are placed at 10.9530 and 12.8427 eV, respectively.

nance has also been obtained theoretically by Sadeghpour, Greene, and Cavagnero [18], although the height of the resonance peak reported by these authors is much smaller than the present one.

The broad structure just above $N=2$ is the well-known shape resonance of H^-. An important point is that the low-energy tail of this resonance peak extends under the $N=2$ threshold, thus contributing to the background observed in that region.

In Fig. 1 one can also see the first Feshbach resonance converging to the $N=3$ threshold, and a mesh of resonant structures just below it. Only the first and the fourth ones have been observed experimentally [8,9].

The partial $N=1$ and $N=2$ cross sections are displayed in Fig. 2. In the shape resonance region, the $N=1$ cross section is much smaller than the $N=2$ one, except very close to the threshold where $\sigma_{N=2}\rightarrow 0$. This is in agreement with the recent experimental results of Halka *et al.* [7] and other theoretical calculations [13,15,18]. At higher energies, $\sigma_{N=2}$ decreases slowly, and at $\simeq 11.3$ eV is comparable to $\sigma_{N=1}$. This holds up to the $N=3$ threshold, except in the region of the Feshbach resonances, where both partial cross sections oscillate.

In order to analyze our results near the resonance structures and to perform an adequate comparison with the available experimental data, we will consider separately the regions near the $N=2$ and $N=3$ thresholds. In both regions we will also separate the $2s$ and $2p$ contributions to $\sigma_{N=2}$.

B. Cross sections near $N=2$

In Fig. 3 we show our results for the $1s$, $2s$, and $2p$ cross sections. From this figure, we see that the residual hydrogen atom is left preferentially in a $2p$ excited state. The ratio between the maxima of the $2p$ and $2s$ cross sections is $\simeq 4$, which is in qualitative agreement with Hyman, Jacobs, and Burke [13], Liu, Du, and Starace [16], and the results of Sadeghpour, Greene, and Cavagnero reported in Fig. 2 of Ref. [7].

We compare in Fig. 4 the $N=2$ cross sections with the available experimental data [7]. The experimental cross sections are given in arbitrary units, so that they have been normalized to the theoretical amplitude. The general agreement is very good. The shape, position, and magnitude of $\sigma_{N=2}$ are also in good agreement with the results of Sadeghpour, Greene, and Cavagnero [18] and Broad and Reinhardt [15]. On the other hand, the resonance peak obtained by Liu, Du, and Starace [16] is broader and $\simeq 2$ times lower than the present one, and is shifted $\simeq 20$ meV up in energy. Finally, the theoretical results of Hyman, Jacobs, and Burke [13] predict a much broader resonance peak, $\simeq 30$ meV higher in energy.

In Fig. 5 we compare the total cross sections with the

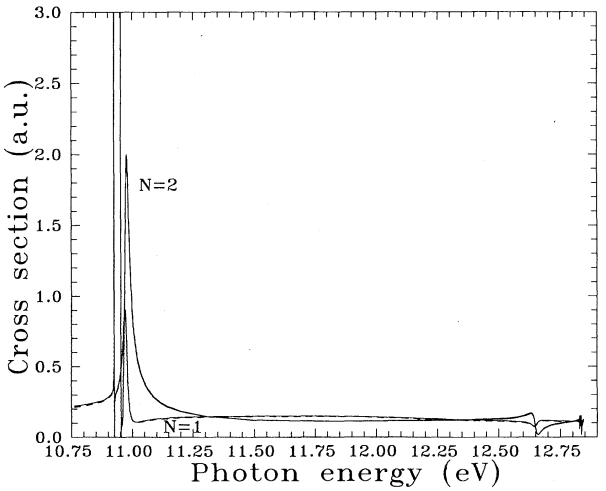

FIG. 2. Partial $\sigma_{N=1}$ and $\sigma_{N=2}$ photodetachment cross sections of H^-. ——, length gauge; — — —, velocity gauge. The $N=2$ and $N=3$ thresholds are placed at 10.9530 and 12.8427 eV, respectively.

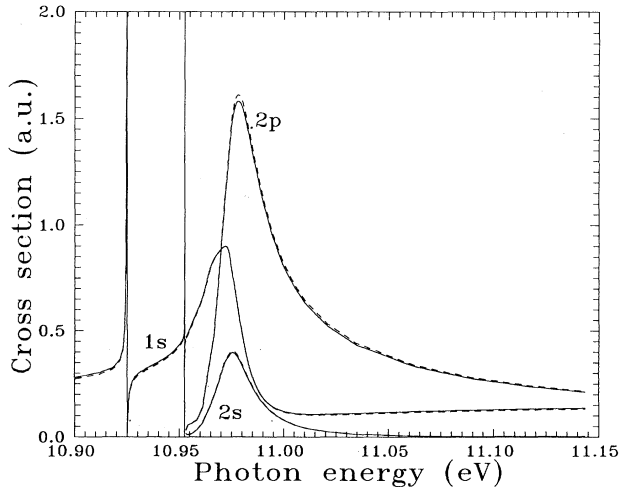

FIG. 3. Partial σ_{1s}, σ_{2s}, and σ_{2p} photodetachment cross sections of H^- in the vicinity of the $N=2$ threshold at 10.9530 eV [7]. ——, length gauge; — — —, velocity gauge.

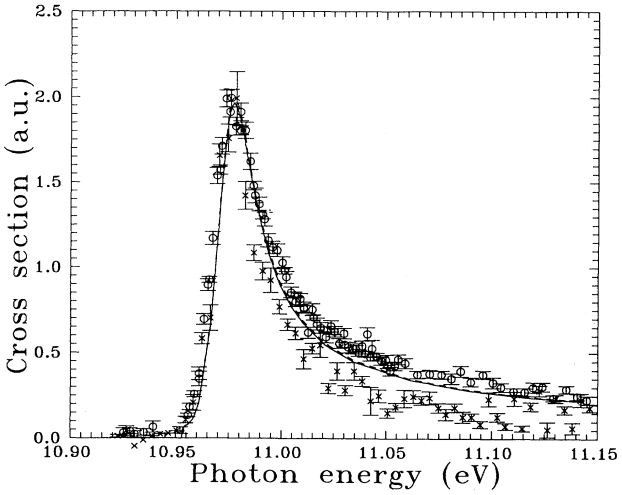

FIG. 4. Comparison between the calculated $\sigma_{N=2}$ cross section and the experimental values of Halka *et al.* [7] (×) and Butterfield reported in [7] (○) in the vicinity of the $N=2$ threshold at 10.9530 eV. The experimental data, obtained in arbitrary units, have been normalized to the theoretical amplitude at the maximum of the cross section. ——, length gauge; — — —, velocity gauge.

experimental ones [5,7]. As in the previous comparison, the experimental values have been normalized to the theoretical amplitude of the shape resonance. The positions of both the first Feshbach resonance below $N=2$ and the shape resonance are in excellent agreement with the experimental ones, and with the theoretical calculations of Refs. [15,18].

Recently, McCarthy and Shang [45] have suggested the existence of another $^1P^o$ resonance state in e^-+H

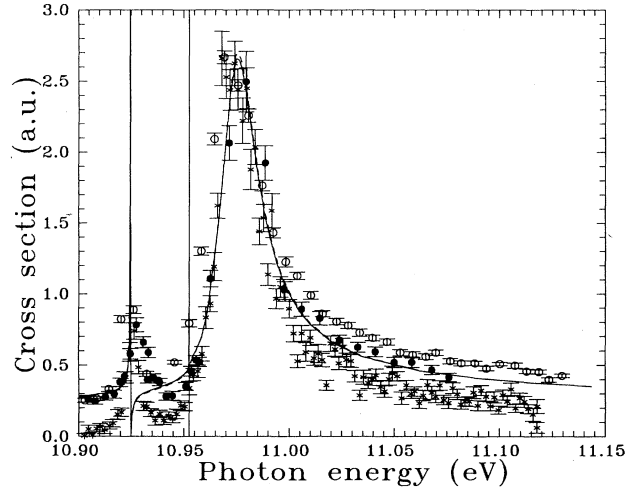

FIG. 5. Comparison between the calculated total cross section and the experimental values of Bryant *et al.* [5] (●), Halka *et al.* [7] (×), and Butterfield reported in [7] (○) in the vicinity of the $N=2$ threshold at 10.9530 eV. The experimental data, obtained in arbitrary units, have been normalized to the theoretical amplitude at the maximum of the cross section just above $N=2$. ——, length gauge; — — —, velocity gauge.

scattering that has been hitherto undetected at lower energies. Explicit photodetachment calculations in this region do not show any resonance structure, in agreement with the recent work of Brage, Froese-Fischer, and Miecznik [28].

C. Cross sections near $N=3$

In Fig. 6 we have plotted the $1s$, $2s$, and $2p$ partial cross sections near $N=3$. The σ_{1s} and σ_{2p} cross sections are roughly comparable, and larger than the σ_{2s} one, except in the vicinity of the resonances. This is more clearly illustrated in Fig. 7 where we have plotted the branching ratio $R(2p:2s)$. This figure is in qualitative agreement with the calculations of Burkov, Letyaev, and Strakhova [17], but these authors predict $R(2p:2s)\simeq 8$ outside the resonance regions.

Figures 6 and 7 show clearly the existence of, at least, two series of resonances. We will use the (K,T) quantum numbers [46] to label them. The first series, (1,1), includes the first and the fourth resonances at 12.66 and 12.84 eV, which are the largest ones. The second series, (2,0), includes at least the two narrow resonances at 12.76 and 12.83 eV. This is in agreement with Sadeghpour, Greene, and Cavagnero [18]. Burkov, Letyaev, and Strakhova [17] have only obtained the two (1,1) resonances and the first (2,0) one. On the other hand, only resonances belonging to the (1,1) series have been observed experimentally [8]. There is still a fifth resonance very close to the $N=4$ threshold, that could be a third member of the (2,0) series, or perhaps a resonance associated to a (0,1) manifold.

We compare in Fig. 8 the $N=2$ cross sections with the experimental values of Halka *et al.* [11], normalized to our background levels. The shape and position of the first broad resonance are in good agreement. $\sigma_{N=2}$ and $\sigma_{N=1}$ are also in good agreement with the R-matrix calculations of Sadeghpour, Greene, and Cavagnero [18].

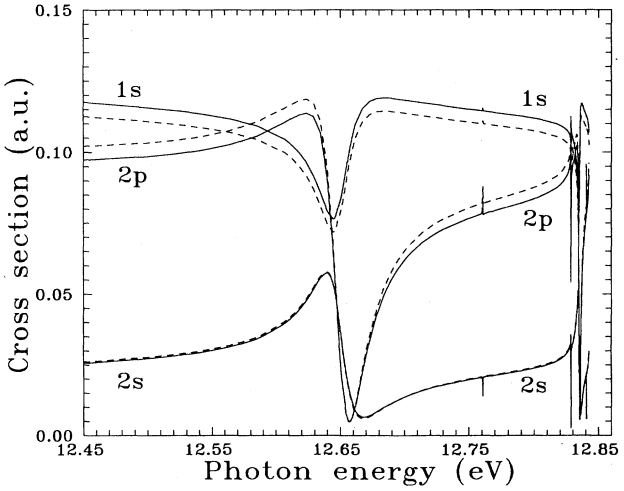

FIG. 6. Partial σ_{1s}, σ_{2s}, and σ_{2p} photodetachment cross sections of H^- in the vicinity of the $N=3$ threshold at 12.8427 eV. ——, length gauge; — — —, velocity gauge.

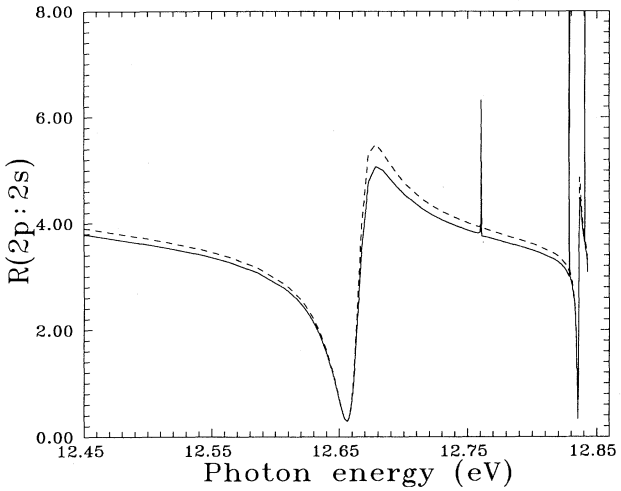

FIG. 7. Branching ratio $R(2p:2s)=\sigma_{2p}/\sigma_{2s}$ of H^- in the vicinity of the $N=3$ threshold at 12.8427 eV. ——, length gauge; — — —, velocity gauge.

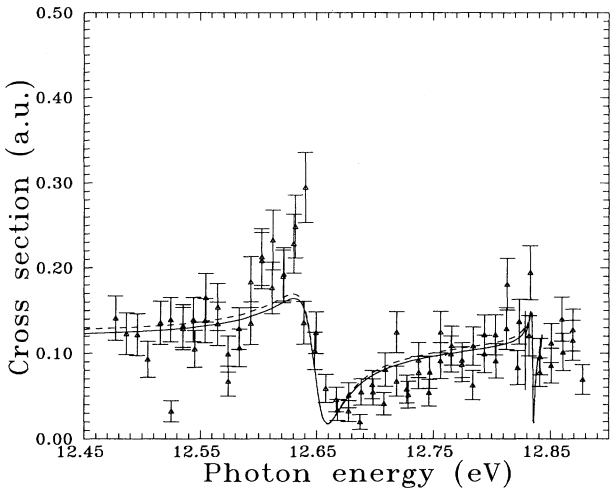

FIG. 8. Comparison between the calculated $\sigma_{N=2}$ cross section and the experimental values of Halka *et al.* [11] (△) in the vicinity of the $N=3$ threshold at 12.8427 eV. The experimental data, obtained in arbitrary units, have been normalized to the theoretical background and shifted 6 meV down in energy, which is within the experimental energy resolution (7 meV) claimed in Ref. [11]. ——, length gauge; — — —, velocity gauge.

Both the shape of the position of the resonances, as well as the magnitude of the cross sections are very similar in both calculations. A minor difference concerns the height of the (2,0) resonance at 12.76 eV, which is almost invisible in Fig. 8. In Ref. [18], this resonance is practically not seen in the velocity gauge (that the authors believe better converged), but it is quite apparent in the length gauge.

The total cross section is compared in Figs. 9(a), and 9(b), with the experimental values of Cohen *et al.* [9] and Hamm *et al.* [8]. Both sets of data have been matched to our theoretical background. Although the overall agreement is reasonable, there is a slight discrepancy in the height of the maximum of the first Feshbach resonance. This discrepancy also exists when comparing with the results of Sadeghpour, Greene, and Cavagnero [18]. However, the magnitude of the cross section and all the resonance positions are in excellent agreement in the two calculations. Hamm *et al.* [8] have performed a finer scanning in the region of the fourth resonance around 12.84 eV. In Fig. 9(c) we compare the calculated cross section with the corresponding experimental data. In this case the limited experimental energy resolution produces a smoothing of the oscillation in the resonance region; however, the width of the resonance structure and its position agree very well with the theoretical results.

D. Resonance parameters

As shown by Fano [20], the total cross section can be parametrized in the vicinity of each resonance using the formula

$$\sigma(E)=\sigma^0\left[\rho_s^2\frac{(q_s+\epsilon)^2}{1+\epsilon^2}+1-\rho_s^2\right], \tag{10}$$

where $\epsilon=2[E-\mathcal{E}_s-\Delta_s(\mathcal{E}_s)]/\Gamma_s(\mathcal{E}_s)$, σ^0 is the background nonresonant cross section, q_s is the line profile parameter, and ρ_s^2 is the correlation parameter ($\rho_s^2=1$ for the case of a single open channel). The partial cross sections can be parametrized following Starace [34]:

$$\sigma_\mu(E)=\frac{\sigma_\mu^0}{1+\epsilon^2}\{\epsilon^2+2\epsilon(q_s\mathrm{Re}[\alpha_\mu^s]-\mathrm{Im}[\alpha_\mu^s])+1-2q_s\mathrm{Im}[\alpha_\mu^s]-2\,\mathrm{Re}[\alpha_\mu^s]+(q_s^2+1)|\alpha_\mu^s|^2\}\ , \tag{11}$$

where σ_μ^0 is the partial background nonresonant cross section and α_μ^s are the Starace parameters. Obviously, this equation reduces to the Fano one when there is only one open channel. As shown by Sánchez and Martín [38], Eq. (1) leads to Eqs. (10) and (11) in the neighborhood of each Feshbach resonance s, provided that the corresponding ϕ_s state is singled out to build the continuum wave function of Eq. (1). Therefore, no fitting procedure is needed to evaluate the resonance parameters, which are directly obtained for $E=\mathcal{E}_s$. These parameters remain practically constant around $\mathcal{E}_s$, and take into account the effect of neighboring resonances through the terms including the $G_Q^{(s)}(E)$ operator. In the present work, we have used the equations reported in Ref. [38] in the length gauge to evaluate the Fano and Starace parameters for the Feshbach resonances lying just below the $N=2$ and $N=3$ threshold.

The shape resonance cannot be treated in the same way

because there is no ϕ_s state that could be attributed to it (see Sec. II). Therefore, in this particular case, we have followed the usual procedure of fitting the cross sections by using a least-squares method. We have made the usual assumption that the background cross sections σ^0 and σ_μ^0 remain practically constant in the resonance region and almost coincide with the actual cross sections outside this region. Consequently, we have chosen for the values of σ^0 and σ_μ^0 those of the corresponding cross sections at 11.20 eV. For the total cross section, the remaining Fano parameters ($\mathcal{E}_s+\Delta_s$, Γ_s, q_s, and ρ_s^2) have been varied without any further restriction. For partial cross sections, the Fano parameters obtained in the previous step have been frozen, and only the Starace parameters α_μ^s have been varied, subject to the following condition [34]:

$$\sum_\mu |\alpha_\mu^s|^2\sigma_\mu^0=\sigma^0\rho_s^2 \ . \tag{12}$$

The partial autoionization widths are then obtained from [34]

$$\Gamma_\mu^s=|\alpha_\mu^s|^2\sigma_\mu^0\Gamma_s(\sigma^0\rho_s^2)^{-1} \ . \tag{13}$$

In Tables I and II we present our results for the resonances lying in the vicinity of the $N=2$ threshold. Previous reported values [6,7,14,18,21,23–27,30,44,47,48] are also included in these tables for comparison. Tables I and II show very good agreement with previous theoretical and experimental determinations of the position and the width of the lowest Feshbach resonance and the shape one. Our calculated q_s parameter for the shape

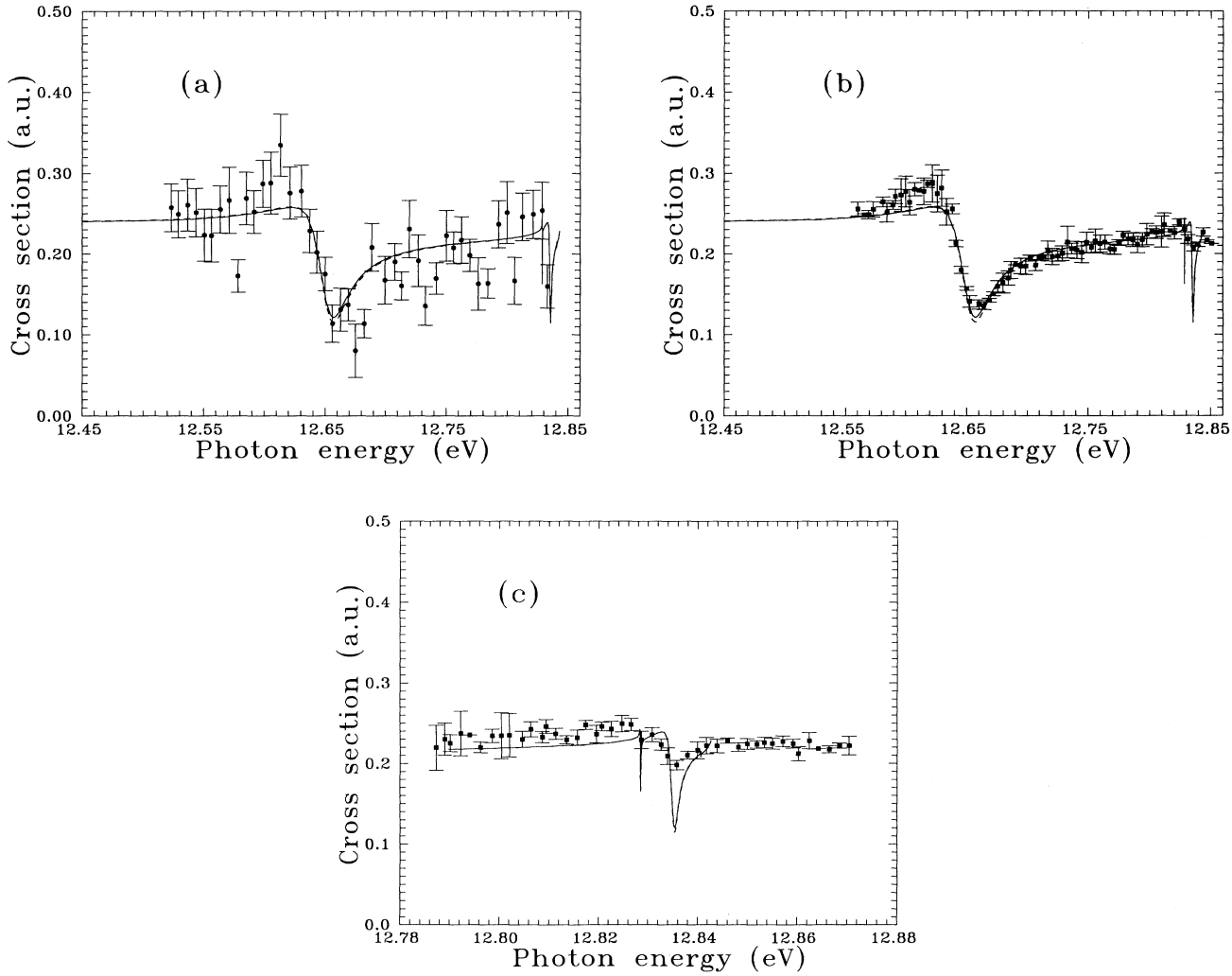

FIG. 9. Comparison between the calculated total cross section and the experimental values of (a) Cohen *et al.* [9] (●) and (b) Hamm *et al.* [8] (■) in the vicinity of the $N=3$ threshold at 12.8427 eV. The experimental data, obtained in arbitrary units, have been normalized to the theoretical background. In (c), we show a comparison of our results with those obtained by Hamm *et al.* [8] (■) by performing a fine scanning in the vicinity of the $4\,^1P^o(1,1)$ resonance; normalization of the experimental data is identical to that used in (b). In (b) and (c), the experimental data have been shifted 6 meV down in energy, which is within the experimental energy resolution (7 meV) claimed in Ref. [8]. ——, length gauge; — — —, velocity gauge.

TABLE I. Energy positions, total autoionization widths, and Fano parameters for the $^1P^o$ doubly excited states of H^- below the $N=2$ threshold. The notation $[-x]$ indicates powers of ten. Each resonance is labeled $k\ ^1P^o(K,T)$, where k indicates energy ordering. The experimental values have been converted to a.u. using the equivalence 1 a.u. = 27.207 952 eV and the experimental electron affinity of H^- 0.754 22 eV [8].

s	Reference	$\mathcal{E}_s+\Delta_s$ (a.u.)	Γ_s (eV)	q_s	σ_s^0 (a.u.)
$1\ ^1P^o$	This work	−0.126 049	0.324[−4]	−15.865	0.288 701
(1,0)	Greene, and Cavagnero [18]	−0.126 014	0.288[−4]		
	Taylor and Burke [21]	−0.126 01	0.4[−4]		
	Wendolowski and Reinhardt [23]	−0.126 048	0.103[−4]		
	Conneely and Lipsky [24]	−0.126 026 9	0.313085[−4]		
	Macías and Riera [25]	−0.126 098	0.14[−4]		
	Pathak, Kingston, and Berrington [26]	−0.126 043			
	Abrashkevich *et al.* [27]	−0.125 932			
	MacArthur *et al.* [44]	−0.126 13			
	Seiler, Oberoi, and Callaway [47]	−0.125 71	0.2[−4]		
$2\ ^1P^o$	This work	−0.125 035	0.17[−5]	−11.632	0.427 514
(1,0)	Abrashkevich *et al.* [27]	−0.125 022			

resonance is also in agreement with the experimental value of Halka *et al.* [7]. It can be observed in Table II that autoionization of the shape resonance to the $N=1$ channel is only 17% of the total autoionization probability. The dominant channel for autoionization is the $2p\epsilon s$ one, followed by the $2p\epsilon d$ channel. Therefore, autoionization of the shape resonance leaves preferentially the remaining hydrogen atom in a $2p$ state.

We consider now the resonances observed near $N=3$. The results are given in Tables III and IV. From Table III, one can observe that the two resonances belonging to the (1,1) series, and those of the (2,0) one, approximately follow the law derived by Gailitis and Damburg [2]:

$$\frac{E_{k+1}-E_{N=3}}{E_k-E_{N=3}}=\frac{\Gamma_{k+1}}{\Gamma_k}=e^{-2\pi/\gamma_j}, \tag{14}$$

where $\gamma_j=\sqrt{-a_j-1/4}$ and a_j is the dipole moment in the j resonance channel, induced by an outer electron on the $N=2$ manifold of a neutral hydrogen atom. We have included the values of such dipole moments in Table III for completeness. Table III also shows that the line profile parameter q_s is negative for all the resonances found in this work and differs very little from one series to another. The values of ρ_s^2 are very similar for the two (1,1) resonances, but differ by two orders of magnitude for the (2,0) ones. The smallness of ρ_s^2 for the first (2,0) resonance explains why it is not observed in the total cross section spectrum.

It is very difficult from the present results to assign the fifth resonance to a particular series. Assuming the validity of the Gailitis-Damburg law [Eq. (7)], this resonance could fit in the (2,0) series. However, we cannot forget

TABLE II. (a) Energy position, total width, and Fano parameters, and (b) partial widths and Starace parameters for the $^1P^o(0,1)$ shape resonance of H^- that lies just above the $N=2$ threshold. The conversion factor relating a.u. to eV is the same of Table I. Numbers within parentheses indicate the uncertainty in the final figures.

(a)

Reference	$\mathcal{E}_s+\Delta_s$ (a.u.)	Γ_s (eV)	q_s	ρ_s^2	σ_s^0 (a.u.)
This work	−0.124 24	0.0226	5.50	0.243	0.322
Bryant *et al.* [6]		0.023(6)			
Halka *et al.* [7]	−0.124 38(1)	0.021(1)	5.3(2)		
Butterfield, as noted in [7]	−0.124 53(1)	0.030(1)	4.5(1)		
Broad and Reinhardt [14]	−0.124 34	0.015			
Sadeghpour, Greene, and Cavagnero [18]	−0.124 242	0.0186			
Wendolowski and Reinhardt [23]	−0.124 351	0.0142			
Pathak, Kingston, and Berrington [26]	−0.124 328	0.0316			
Callaway [31]	−0.124 395	0.0200			
Williams [48]	−0.124 48(7)	0.022(3)			

(b)

μ	σ_μ^0 (a.u.)	Γ_μ^s/Γ_s	Re(α_μ^s)	Im(α_μ^s)
$1s\epsilon p$	0.137	0.175	−0.290	−0.126
$2s\epsilon p$	0.004	0.161	1.795	−0.143
$2p\epsilon s$	0.158	0.437	0.454	0.099
$2p\epsilon d$	0.022	0.227	0.893	0.019

TABLE III. Energy positions, total autoionization widths, and Fano parameters for the $^1P^o$ doubly excited states of H^- below the $N=3$ threshold. The notation $[-x]$ indicates powers of ten. Each resonance is labeled $k\ ^1P^o(K,T)$, where k indicates the energy ordering. a_j is the dipole moment defined after Eq. (14).

s	a_j (a.u.)	$\mathcal{E}_s+\Delta_s$ (a.u.)	Γ_s (eV)	ρ_s^2	q_s	σ_s^0 (a.u.)
$1\ ^1P^o(1,1)$	−5.220	−0.062 646 8	0.275 462[−1]	0.465 047	−0.514 419	0.226 256
$2\ ^1P^o(2,0)$	−14.897	−0.058 569 7	0.193 463[−3]	0.534 852[−2]	−0.495 162	0.213 039
$3\ ^1P^o(2,0)$	−14.897	−0.056 075 9	0.646 631[−4]	0.306 388	−0.414 797	0.230 937
$4\ ^1P^o(1,1)$	−5.220	−0.055 836 7	0.179 021[−2]	0.459 756	−0.405 189	0.222 591
$5\ ^1P^o$		−0.055 629 0	0.806 841[−5]	0.398 261[−1]	−0.700 456	0.212 235

that the asymptotic potential felt by an escaping electron in a (0,1) series is only slightly repulsive, so that it might support doubly excited states.

From an inspection of the partial widths of Table IV, we can conclude that autoionization of these doubly excited states leaves the H^- ion mainly in an $N=2$ excited state, in agreement with the conclusions of Ref. [18]. The hydrogen atom remains preferentially in a $2p$ state for the (1,1) resonances, whereas $2s$ and $2p$ states are approximately equally populated for the remaining resonant states. Another relevant feature of Table IV is the great similarity of the α_μ^s components for the first and the fourth Feshbach resonances, which explains why the partial cross sections behave similarly in the vicinity of such resonances.

We compare in Table V our calculated resonance parameters with previous values reported in the literature. The energy positions and widths are in good agreement with the experimental values of Hamm *et al.* [8], Cohen *et al.* [9], and Halka *et al.* [11]. The agreement is also very good for ρ_s^2. However, the present values for q_s are slightly less negative than the experimental ones, which explains why the maximum of the total cross section in the neighborhood of the (1,1) resonance is smaller than the experimental one.

The energy positions are slightly higher than those of accurate theoretical calculations. Burkov, Letyaev, and Strakhova [17] report energies that are significantly higher than the present ones. Comparison for the widths is good, although most theories predict a slightly larger width for the first Feshbach resonance. Finally, some of our calculated ρ_s^2 and q_s values differ significantly from those reported in Ref. [17].

Finally, in Table VI we have compared our results with the partial widths reported by Chrysos, Komninos, and Nicolaides [33] for the $1\ ^1P^o(1,1)$ resonance state. Both calculations predict that the largest partial width is the $2p\varepsilon s$ one, that hydrogen is left mainly in a $2p$ state after autoionization, and that autoionization to the nearest threshold $N=2$ is much more important than autoionization to $N=1$. However, we obtain that the $2s\varepsilon p$ and $2p\varepsilon d$ partial widths are comparable, whereas Chrysos, Komninos, and Nicolaides [33] find that the $2p\varepsilon d$ one is almost negligible.

TABLE IV. Partial autoionization widths and Starace parameters for the $^1P^o$ doubly excited states of H^- below the $N=3$ threshold. Notation as in Table III.

s	μ	σ_μ^0 (a.u.)	Γ_μ (eV)	$\mathrm{Re}(\sigma_\mu^s)$	$\mathrm{Im}(\alpha_\mu^s)$
$1\ ^1P^o(1,1)$	$1s\varepsilon p$	0.113 974	0.976 193[−3]	0.783 41[−1]	−0.163 03
	$2s\varepsilon p$	0.024 354	0.514 780[−2]	0.569 57	0.694 97
	$2p\varepsilon s$	0.055 858	0.168 595[−1]	1.069 86	−0.911 21[−1]
	$2p\varepsilon d$	0.032 071	0.456 278[−2]	0.706 54	0.210 34
$2\ ^1P^o(2,0)$	$1s\varepsilon p$	0.114 456	0.286 185[−6]	−0.349 56[−2]	0.158 36[−2]
	$2s\varepsilon p$	0.020 577	0.810 892[−4]	0.122 14	−0.910 58[−1]
	$2p\varepsilon s$	0.049 713	0.662 468[−4]	−0.738 38[−2]	0.882 84[−1]
	$2p\varepsilon d$	0.028 292	0.458 406[−4]	−0.214 44[−1]	−0.953 05[−1]
$3\ ^1P^o(2,0)$	$1s\varepsilon p$	0.106 014	0.923 476[−6]	0.153 24[−1]	−0.964 21[−1]
	$2s\varepsilon p$	0.031 085	0.288 936[−4]	1.007 55	−0.441 19[−1]
	$2p\varepsilon s$	0.057 703	0.238 292[−4]	0.450 42	0.499 00
	$2p\varepsilon d$	0.036 136	0.110 169[−4]	0.327 16	−0.475 99
$4\ ^1P^o(1,1)$	$1s\varepsilon p$	0.109 578	0.650 261[−4]	0.669 80[−1]	−0.171 57
	$2s\varepsilon p$	0.026 319	0.302 614[−3]	0.521 72	0.620 54
	$2p\varepsilon s$	0.054 124	0.108 689[−2]	1.065 96	−0.108 19
	$2p\varepsilon d$	0.032 570	0.335 680[−3]	0.723 77	0.255 58
$5\ ^1P^o$	$1s\varepsilon p$	0.112 703	0.427 285[−8]	−0.434 10[−2]	−0.456 87[−2]
	$2s\varepsilon p$	0.021 556	0.339 506[−5]	0.369 53	−0.168 65
	$2p\varepsilon s$	0.049 795	0.270 180[−5]	0.400 62[−1]	0.235 02
	$2p\varepsilon d$	0.028 182	0.196 728[−5]	−0.361 50[−1]	−0.268 00

TABLE V. Comparison between our calculated resonant parameters and other theoretical and experimental results. The latter have been converted to a.u. using the equivalence 1 a.u.=27.207 952 eV and the experimental electron affinity of H^- 0.754 22 eV [8]. We have used the equivalence 1 a.u.=28.0028 Mb to convert the background cross sections of Ref. [17] to a.u. Numbers within parentheses indicate the uncertainty in the final figures. Resonances are labeled as in Table III.

s	Reference	$\mathcal{E}_s+\Delta_s$ (a.u.)	Γ_s (eV)	ρ_s^2	q_s	σ_s^0 (a.u.)
$1\,^1P^o$	This work	−0.062 646 8	0.02755	0.465 05	−0.514 42	0.226 26
(1,1)	Hamm *et al.* [8]	−0.062 78(15)	0.0275(8)	0.440(18)	−0.81(8)	
	Cohen *et al.* [9]	−0.062 78(4)	0.039(2)	0.479(98)	−0.7169(372)	
	Halka *et al.* [11]	−0.062 70(11)	0.030(3)			
	Burkov, Letyaev, and Strakhova [17]	−0.062 25	0.0379	0.466	−1.040	0.2292
	Sadeghpour, Greene, and Cavagnero [18]	−0.062 695	0.0334			
	Pathak, Kingston, and Berrington [26]	−0.062 713	0.0342			
	Callaway [31]	−0.062 72	0.0324			
	Ho [32]	−0.062 716 8	0.03242			
$2\,^1P^o$	This work	−0.058 569 7	0.000 19	0.005 35	−0.495 16	0.213 04
(2,0)	Burkov, Letyaev, and Strakhoava [17]	−0.058 39	0.000 26	0.128	−3.469	0.2217
	Sadeghpour, Greene, and Cavagnero [18]	−0.058 866	0.000 403			
	Pathak, Kingston, and Berrington [26]	−0.058 572	0.000 245			
	Callaway [31]	−0.058 57	0.000 245			
	Ho [32]	−0.058 571 8	0.000 244 6			
$3\,^1P^o$	This work	−0.056 075 9	0.000 065	0.306 39	−0.414 80	0.230 94
(2,0)	Pathak, Kingston, and Berrington [26]	−0.056 145				
	Callaway [31]	−0.056 12	0.000 059 3			
	Ho [32]	−0.056 116 7	0.000 057			
$4\,^1P^o$	This work	−0.055 836 7	0.001 79	0.459 76	−0.405 19	0.222 59
(1,1)	Hamm *et al.* [8]	−0.055 91(15)	0.001 6(3)	0.424(76)	−0.67(14)	
	Burkov, Letyaev, and Strakhova [17]	−0.055 86	0.001 58	0.534	−0.635	0.2541
	Sadeghpour, Greene, and Cavagnero [18]	−0.055 832	0.001 16			
	Pathak, Kingston, and Berrington [26]	−0.055 903	0.001 81			
	Callaway [31]	−0.055 90	0.001 86			
	Ho [32]	−0.055 907	0.0019			

IV. CONCLUSIONS AND FINAL REMARKS

In this paper we have presented total and partial photodetachment cross sections of H^- in the vicinity of the $N=2$ and $N=3$ thresholds. We have used a fully L^2 method, recently proposed in the literature [35], to describe continuum wave functions. It was specially designed for the case of strong interchannel coupling, so that the H^- ion is a good candidate to further test its potentiality. In this method we handle separately the resonant and the nonresonant contributions to the wave function by defining, respectively, orthogonal Q and P subspaces, and we use the Feshbach theory to rebuild the continuum state as described by Sánchez and Martín [38]. An advantage of this approach is that it leads naturally to the Fano and Starace parametrizations of total and partial cross sections in the vicinity of the Feshbach resonances. On the other hand, shape resonances remain in P subspace together with the nonresonant components, so that the way of partitioning the whole space into P and Q subspaces is irrelevant in this case.

The Q components of the wave function are obtained in a basis of STO's in the framework of the pseudopotential-Feshbach method [42], which is mathematically equivalent to the standard Feshbach one, but it is more easily implemented when using large basis sets above several ionization thresholds.

The P components of the wave function are evaluated with an L^2 basis in the following way. For each channel, the nonresonant Green function is calculated in a representation of orthogonal uncoupled continuum states built from STO's. Discretization of the latter continuum states

TABLE VI. Percentage of the partial autoionization widths to the total ones for the first $^1P^o(1,1)$ resonance of H^- below $N=3$. The comparison is between our results and those of Chrysos, Komninos, and Nicolaides [33].

		Γ_μ^s	
s	μ	This work	Chrysos, Komninos, and Nicholaides [33]
$1\,^1P^o$ (1,1)	$1s\varepsilon p$	3.5%	0.0%
	$2s\varepsilon p$	18.7%	39.7%
	$2p\varepsilon s$	61.2%	60.0%
	$2p\varepsilon d$	16.6%	0.3%

is trivial and can be performed by using any standard technique published in the literature for the case of a single open channel. In particular, we have used the procedure of Macías *et al.* [43] which makes use of an even-tempered basis of STO's. An important requirement is that the discretized spectrum for each uncoupled channel is smooth (see Ref. [43] for a quantitative prescription) in order to perform a correct quadrature of the energy integrals, and to obtain the proper renormalization factor to achieve the δ-function normalization. The smoothness of the discretization is automatically guaranteed following the instructions of Ref. [43], provided that Feshbach resonances have been projected out to the complementary subspace Q. However, this property must be checked in the regions where there are shape resonances, as in H^-.

The origin of the shape resonance of H^- is a strong configuration mixing between $2lkl'$ configurations. Use of a single type of configurations does *not* provide stable eigenvalues in P subspace that would permit the identification of shape resonances. This has been proven unambiguously by Cortés *et al.* [49] in a previous work. Therefore, our uncoupled representations of the continuum states present *no* resonant behavior in the shape resonance region, and, therefore, they all verify the smoothness requirement. Then it is very nice to see how inclusion of interchannel coupling in P subspace through the corresponding Green function reveals the presence of the shape resonance in the photodetachment cross sections.

Our results for total and partial $N=1$ and $N=2$ cross sections are in good agreement with the experimental data, and with the most extensive theoretical calculations performed up to date [18]. In particular, we have obtained the two Feshbach resonances that lie below $N=2$, the shape resonance just above this threshold, and five Feshbach resonances converging to the $N=3$. From the latter, the first and the fourth belong to the (1,1) series, the second and the third to the (2,0) one, and the fifth has not been clearly classified. Also we have found that the remaining hydrogen atom is left preferentially in an $N=2$ excited state up to photon energies $\simeq 11.3$ eV.

It should be pointed out that the major theoretical difficulty in evaluating cross sections in the shape resonance region is the importance of describing properly the interchannel coupling just above threshold. Then, the good agreement found between the present results and the experimental ones constitutes a very stringent test of the L^2 technique developed in Ref. [35].

We have presented the separate contribution of the partial $2s$ and $2p$ cross sections to the $N=2$ one. In the whole energy region considered in this work, the $2p$ cross section is larger than the $2s$ one, especially in the shape resonance region.

Finally, we have obtained energy positions, total and partial autoionization widths, and Fano and Starace parameters for the resonances lying in the vicinity of the $N=2$ and $N=3$ thresholds, including the shape resonance. This is a useful information to interpret the resonance structures observed in the photodetachment spectrum and to understand the autoionization properties of the doubly excited states. We have found that energy positions and total widths roughly follow the Gailitis-Damburg law [2] for each series of resonances, and that autoionization leaves the hydrogen atom in an $N=2$ excited state, which is preferentially a $2p$ state for the (1,1) series. All the Feshbach resonances observed in the photodetachment spectra have a negative line profile parameter q_s. Therefore, one can tentatively state that the attractive nature of the long-range dipole potential acting upon the escaping electron in the presence of a neutral hydrogen atom seems to be related with a negative sign for q_s. However, this is a point that should be further investigated.

ACKNOWLEDGMENTS

This work has been partially supported by the DGICYT Project No. PB90-213 and the EEC Twining Program No. SCI*.0138.C(JR).

[1] M. J. Seaton, Proc. Phys. Soc. London **77**, 174 (1961).
[2] M. Gailitis and R. Damburg, Proc. Phys. Soc. London **82**, 192 (1963).
[3] J. Macek and P. G. Burke, Proc. Phys. Soc. London **92**, 351 (1967).
[4] D. R. Herrick, Phys. Rev. A **12**, 413 (1975).
[5] H. C. Bryant, B. D. Dieterle, J. Donahue, H. Sharifian, H. Tootoonchi, D. M. Wolfe, P. A. M. Gram, and M. A. Yates-Williams, Phys. Rev. Lett. **38**, 228 (1977).
[6] H. C. Bryant, D. A. Clark, K. B. Butterfield, C. A. Frost, H. Sharifian, H. Tootoonchi, J. B. Donahue, P. A. M. Gram, M. E. Hamm, R. W. Hamm, J. C. Pratt, M. A. Yates, and W. W. Smith, Phys. Rev. A **27**, 2889 (1983).
[7] M. Halka, H. C. Bryant, C. Johnstone, B. Marchini, W. Miller, A. H. Mohagheghi, C. Y. Tang, K. B. Butterfield, D. A. Clark, S. Cohen, J. B. Donahue, P. A. M. Gram, R. W. Hamm, A. Hsu, D. W. MacArthur, E. P. MacKerrow, C. R. Quick, J. Tiee, and K. Rózsa, Phys. Rev. A **46**, 6942 (1992).
[8] M. E. Hamm, R. W. Hamm, J. Donahue, P. A. M. Gram, J. C. Pratt, M. A. Yates, R. D. Bolton, D. A. Clark, H. C. Bryant, C. A. Frost, and W. W. Smith, Phys. Rev. Lett. **43**, 1715 (1979).
[9] S. Cohen, H. C. Bryant, C. J. Harvey, J. E. Stewart, K. B. Butterfield, D. A. Clark, J. B. Donahue, D. W. MacArthur, G. Comtet, and W. W. Smith, Phys. Rev. A **36**, 4728 (1987).
[10] P. G. Harris, H. C. Bryant, A. H. Mohagheghi, R. A. Reeder, C. Y. Tang, J. B. Donahue, and C. R. Quick, Phys. Rev. A **42**, 6443 (1990).
[11] M. Halka, H. C. Bryant, E. P. MacKerrow, W. Miller, A. H. Mohagheghi, C. Y. Tang, S. Cohen, J. B. Donahue, A. Hsu, C. R. Quick, J. Tiee, and K. Rózsa, Phys. Rev. A **44**, 6127 (1991).
[12] J. Macek, Proc. Phys. Soc. London **92**, 365 (1967).
[13] H. A. Hyman, V. L. Jacobs, and P. G. Burke, J. Phys. B **5**, 2282 (1972).
[14] J. T. Broad and W. P. Reinhardt, J. Phys. B **9**, 1491 (1976).
[15] J. T. Broad and W. P. Reinhardt, Phys. Rev. A **14**, 2159 (1976).

[16] C. Liu, N. Du, and A. F. Starace, Phys. Rev. A **43**, 5891 (1991).
[17] S. M. Burkov, N. A. Letyaev, and S. I. Strakhova, Phys. Lett. A **150**, 31 (1990).
[18] H. R. Sadeghpour, C. H. Greene, and M. Cavagnero, Phys. Rev. A **45**, 1587 (1992).
[19] P. G. Burke and W. D. Robb, Adv. At. Mol. Phys. **11**, 134 (1974).
[20] U. Fano, Phys. Rev. **124**, 1866 (1961); U. Fano and J. W. Cooper, *ibid.* **137**, A1364 (1965).
[21] A. Taylor and P. G. Burke, Proc. Phys. Soc. London **92**, 336 (1967).
[22] M. P. Ajmera and K. T. Chung, Phys. Rev. A **10**, 1013 (1974).
[23] J. J. Wendolowski and W. P. Reinhardt, Phys. Rev. A **17**, 195 (1978).
[24] M. J. Conneely and L. Lipsky, J. Phys. B **24**, 4135 (1978).
[25] A. Macías and A. Riera, Europhys. Lett. **2**, 351 (1986).
[26] A. Pathak, A. E. Kingston, and K. A. Berrington, J. Phys. B **21**, 2939 (1988).
[27] A. G. Abrashkevich, D. G. Abrashkevich, M. S. Kashiev, I. V. Puzynin, and S. I. Vinitsky, Phys. Rev. A **45**, 5274 (1992).
[28] T. Brage, C. Froese-Fischer, and G. Miecznik, J. Phys. B **25**, 5289 (1992).
[29] R. S. Oberoi, J. Phys. B **5**, 1120 (1972).
[30] L. Lipsky, R. Anania, and M. J. Conneely, At. Data. Nucl. Data Tables **20**, 127 (1977).
[31] J. Callaway, Phys. Lett. **75A**, 43 (1979); Phys. Rev. A **26**, 199 (1982); **37**, 3692 (1988).
[32] Y. K. Ho, Phys. Lett. **77A**, 147 (1980); Phys. Rev. A **45**, 148 (1992).
[33] M. Chrysos, Y. Komninos, and C. Nicolaides, J. Phys. B **25**, 1977 (1992).
[34] A. F. Starace, Phys. Rev. A **16**, 231 (1977).
[35] F. Martín, Phys. Rev. A **48**, 331 (1993).
[36] H. Feshbach, Ann. Phys. (N.Y.) **19**, 287 (1962).
[37] I. Sánchez and F. Martín, Phys. Rev. A **44**, 13 (1991).
[38] I. Sánchez and F. Martín, Phys. Rev. A **44**, 7318 (1991).
[39] I. Sánchez and F. Martín, Phys. Rev. A **45**, 4468 (1992).
[40] C. L. Pekeris, Phys. Rev. **126**, 1470 (1962).
[41] Y. Hahn, T. F. O'Malley, and L. Spruch, Phys. Rev. **128**, 932 (1962).
[42] F. Martín, O. Mó, A. Riera, and M. Yáñez, Europhys. Lett. **4**, 799 (1987); J. Chem. Phys. **87**, 6635 (1987).
[43] A. Macías, F. Martín, A. Riera, and M. Yáñez, Phys. Rev. A **36**, 4179 (1987); Int. J. Quantum Chem. **33**, 279 (1988).
[44] D. W. MacArthur, K. B. Butterfield, D. A. Clark, J. B. Donahue, P. A. M. Gram, H. C. Bryant, C. J. Harvey, W. W. Smith, and G. Comtet, Phys. Rev. A **32**, 1921 (1985).
[45] I. E. McCarthy and B. Shang, Phys. Rev. A **46**, 3959 (1992).
[46] D. R. Herrick and O. Sinanoglu, Phys. Rev. A **11**, 97 (1975).
[47] G. J. Seiler, R. S. Oberoi, and J. Callaway, Phys. Rev. A **3**, 2006 (1971).
[48] J. F. Williams, J. Phys. B **21**, 2107 (1988).
[49] M. Cortés, A. Macías, F. Martín, and A. Riera, J. Phys. B **25**, 83 (1992).